Journal of Materials Chemistry B

Accepted Manuscript

This article can be cited before page numbers have been issued, to do this please use: S. Palanisamy, X. Zhang and T. He, *J. Mater. Chem. B*, 2015, DOI: 10.1039/C5TB00495K.

ROYAL SOCIETY OF CHEMISTRY

www.rsc.org/materialsB

Journal of Materials Chemistry B

Dynamic Article Links ►
View Article Online
DOI: 10.1039/C5TB00495K

Cite this: DOI: 10.1039/c0xx00000x

www.rsc.org/xxxxxx

Paper

Fast, sensitive and selective colorimetric gold bioassay for dopamine detection

Sivakumar Palanisamy,[a,b] Xuehua Zhang*[a] and Tao He*[a]

Received (in XXX, XXX) Xth XXXXXXXXX 20XX, Accepted Xth XXXXXXXXX 20XX
DOI: 10.1039/b000000x

Colorimetric detection of dopamine has the advantage of simplicity in operation and instrumentation. Herein, a highly sensitive and selective colorimetric biosensor with fast response has been developed by using 4'-aminobenzo-18-crown-6 (ABCE) and 4-mercaptophenyl boronic acid (MPBA) modified Au nanoparticles. The modified probe shows an excellent detection limit of 6.0 nM of dopamine at S/N of 2.01 and about 46 nM at S/N of 3 within microseconds response. It exhibits excellent detection selectivity even in 1000-fold excess of many different interferents like metal ions, uric acid and ascorbic acid. All these may make them fulfill the requirements for *in-vivo* analysis.

1. Introduction

Biogenic amine of dopamine (DA) plays an important role in health and disease. *In-vivo* DA concentration is used as clinical indicator for a wide range of illnesses, including tumors of neural crest, cardiovascular disease, and neuromuscular disorder.[1] DA level in the body fluids ranges from several 0.01 to 1 μM.[2] So it is a great challenge in brain science to detect DA at low concentrations with high selectivity, also due to the co-existence of plenty of interferents. Many methods have been employed to probe the DA and its metabolites hitherto. The widely used ones include electrochemical,[3] chemiluminescent,[4] spectrometric,[5] fluorometric[6] and chromatographic methods.[7]

Colorimetric methods have attracted much attention recently for bio-molecular detection by using gold (Au) and silver (Ag) nanoparticles (NPs).[8–10] Their extremely high extinction coefficient and strong dependence of optical properties on the particle size, shape and distance allow the Au and Ag NPs to be utilized as an ideal color indicator. For instance, the molar extinction coefficient is 2.7×10^8 and 1.5×10^{10} M^{-1} cm^{-1} (at ~ 520 nm) for 13 and 50 nm Au NPs, respectively,[11] which is 3–5 orders larger than that of traditional organic compounds. The color of Au suspension changes from red to blue due to the red-shift in the surface plasmon band when Au NPs approach each other and start to aggregate. Thus, Au NPs even at nanomolar concentration can be used for ultrasensitive detection with minimal consumption of materials.

The major requirement of these colorimetric biosensors is the selection of proper specific ligands, which should have high affinity to the specific bio-recognition with DA, since the sensing is based on the aggregation of Au NPs. It has been reported that the Au NPs modified by 4-amino-3-hydrazino-5-mercapto-1,2,4-triazol (AHMT) exhibit a limit of detection (*LOD*) about 70 nM DA (*S/N* ~ 3).[12] Though such Au colorimetric probes have good sensitivity for DA detection, the selectivity is the major concern in the presence of interferents (such as ascorbic acid (AA), uric acid (UA), glucose, and the like), as they can interact with the ligand molecules too. Considering the boronic acid derivatives can be employed as the ligands for some chemosensors,[13-18] they have been used to functionalize the Au NPs as specific ligands for the catechol group of DA, together with 4-(dimethylamino) pyridine or dithiobis(succinimidylpropionate) (DSP) as the specific ligands for the amine group of DA.[19-21] Such probes show a high *LOD* at nanomolar levels, as well as good selectivity. Specifically, they have been successfully applied for the DA detection in the artificial cerebrospinal fluid,[20] and even in the rat brain.[21] But it is noted that these dual molecular recognition probes exhibit relatively slow response time for DA detection in minutes, or even in tens of minutes. This cannot fulfill the requirements for *in-vivo* analysis.

To develop a highly sensitive and selective colorimetric assay with fast response, therefore, in this work we developed three different Au probes by using different ligands. The pyridine-4-boronic acid (PDBA) or 4-mercapto phenyl boronic acid (MPBA) was used as the specific ligand for the catechol group of DA, and DSP or 4'-aminobenzo-18-crown-6 (ABCE) as the specific ligand for the amine group of DA. The obtained best probe exhibited high detection sensitivity at nanomolar level and high selectivity, as well as fast response time in tens of milliseconds (ms).

View Article Online
DOI: 10.1039/C5TB00495K

2. Experimental section

2.1 Materials

Dopamine hydrochloride (DA), ascorbic acid (AA), uric acid (UA), 4-mercapto phenylboronic acid (MPBA), pyridine-4-boronic acid (PDBA), dithiobis succinimidyl propionate (DSP) and 4'-aminobenzo-18-crown-6 (ABCE) were purchased from Sigma Aldrich. L-3-(3,4-dihydroxyphenyl)alanine (LD) and epinephrine hydrochloride were bought from J&K Scientific Ltd.. Chloroauric acid ($HAuCl_4 \cdot 4H_2O$), sodium citrate and nitrate salts were bought from Sino pharma industries. Unless otherwise specified, all the chemical reagents and solvents used were of analytical reagent grade and the solutions were prepared using Milli–Q water (18.2 MΩ·cm).

2.2 Bioassay fabrication

Colloidal Au NPs were synthesized by already reported procedure.[22] The particles with an average diameter of 15 nm were prepared by adding 10 mL of 38.8 mM sodium citrate into 100 mL of 1 mM $HAuCl_4$ under boiling condition with vigorous stirring. The colloidal suspension was cleaned with centrifugation under 10,000 rpm for 5 min, and then filtrated through a 0.2 μm membrane filter to remove the excess salts and the large particles. The as-synthesized Au NPs were confirmed by UV-vis absorption spectra with the absorption wavelength at 514 nm. Then the obtained Au NPs were used to prepare three different Au nanoprobes by replacing the citrate ligands via adding 2 mL of target ligand molecules into 100 mL of citrate capped Au suspension. i.e., 1 mM PDBA and 0.5 mM DSP for Au@PDBA-DSP (Probe 1), 1 mM PDBA and 0.01 mM ABCE for Au@PDBA-ABCE (Probe 2), and 0.01 mM MPBA and 0.01 mM ABCE for Au@MPBA-ABCE (Probe 3). No obvious color change was observed during this ligand-exchange process. After Au NPs were modified through the ligand-exchange process, the modified Au NPs were purified through dialysis in Milli–Q water for at least 12 h.

2.3 Instrumentation

The UV-vis absorption spectra were collected on an UV-vis-NIR spectrophotometer (Perkin Elmer, Lambda 750). The FT-IR spectra were recorded on Spectrum One B Fourier-transform infrared spectroscopy. The dynamic light scattering (DLS) spectra were measured on Malvern Zetasizer Nano Z so as to determine the particle size and zeta potential distribution. The morphology of obtained NPs and related aggregations were characterized by a Tecnai G_2 20 S–TWIN transmission electron microscope (TEM). The colorimetric visualization was carried out with photographs captured by a Canon power shot SD800 IS digital camera.

3. Results and discussion

Three different Au nanoprobes have been prepared by replacing the citrate ligands with target ligands so as to study the sensitivity, selectivity and response time of DA detection, as shown in Scheme 1. The FT-IR spectra for Au coated with citrate, different ligands (DSP, PDBA, ABCE and MPBA), and different nanoprobes are shown in Figure 1, as well as in Supporting Information (Table S1-S3). Two characteristic peaks at 1644 cm^{-1} (C=O stretch mode) and 1400 cm^{-1} (C–O asymmetric stretch mode) can be clearly observed in the spectrum for the Au NPs coated with citrate groups, while they cannot be observed in the spectra for all the three nanoprobes. The spectra for all of the nanoprobes show the characteristic peak of vibration mode for benzene ring (from ABCE and MPBA) or pyridine (from PDBA) at ~1633 cm^{-1}. Moreover, the spectrum for Probe 1 exhibits the characteristic peak at 1260 cm^{-1} (N–O) from DSP ligand, and the spectra for Probes 2 & 3 have the characteristic peak at 1073 cm^{-1} (CH_2CH_2O vibration mode) from ABCE ligand. Thus, all of the target ligands have been successfully grafted onto the Au NPs, indicating successful fabrication of the target nanoprobes.

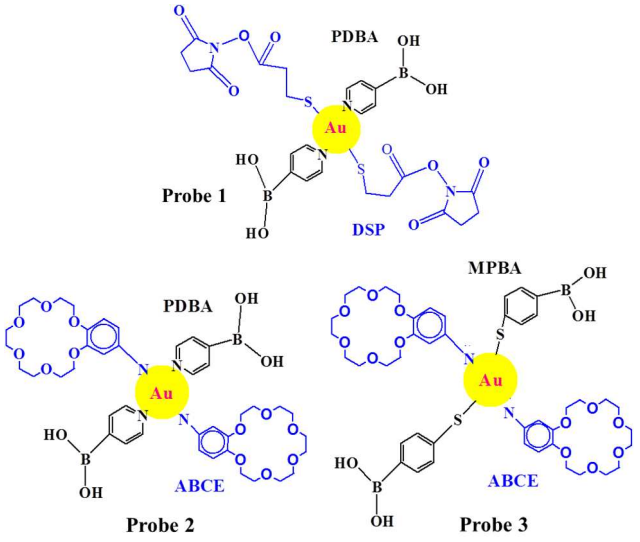

Scheme 1 Au NPs functionalized by dual molecular ligands for colorimetric detection of DA: Au@PDBA-DSP, Au@PDBA-ABCE and Au@MPBA-ABCE.

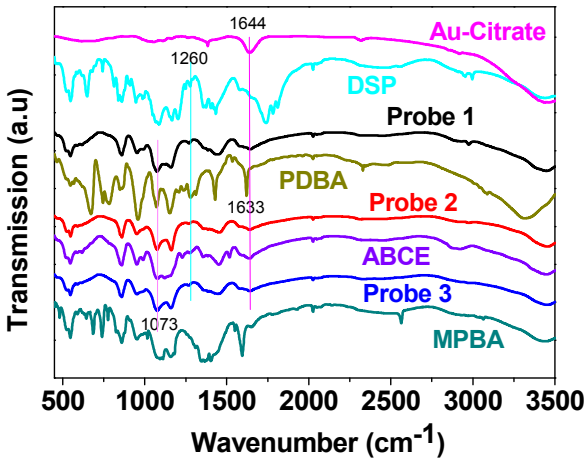

Fig. 1 FT-IR spectra of Au NPs capped with citrate, PDBA, DSP, ABCE and MPBA, as well as spectra of Probes 1, 2 and 3.

3.1 Colorimetric detection of DA

To investigate the detection properties of the obtained nanoprobes, a series of 20 μL of 0.15 to 45 μM DA aqueous solutions were

View Article Online
DOI: 10.1039/C5TB00495K

added into the corresponding individual vials containing 3 mL of Au nanoprobe (eventually 1 to 300 nM of DA, details are given in the Supporting Information). The obtained suspensions were shaken well using vortex shaker before any further characterizations. Besides the visualization pictures, the color change was monitored by the UV-vis absorption spectra for the colorimetric detection. The color of all the as-prepared nanoprobes was wine red and exhibited an absorption peak at 514 nm (Figure 2), which is the typical surface plasmon resonance (SPR) transverse mode for monodispersed spherical Au NPs. The wavelength of this absorption peak is closely related to the free electron density (N_e), as shown in Equation 1, where ω_p is bulk plasma frequency of metal NPs.[23]

$$\omega_p = (N_e^2/m\varepsilon_0)^{1/2} \quad (1)$$

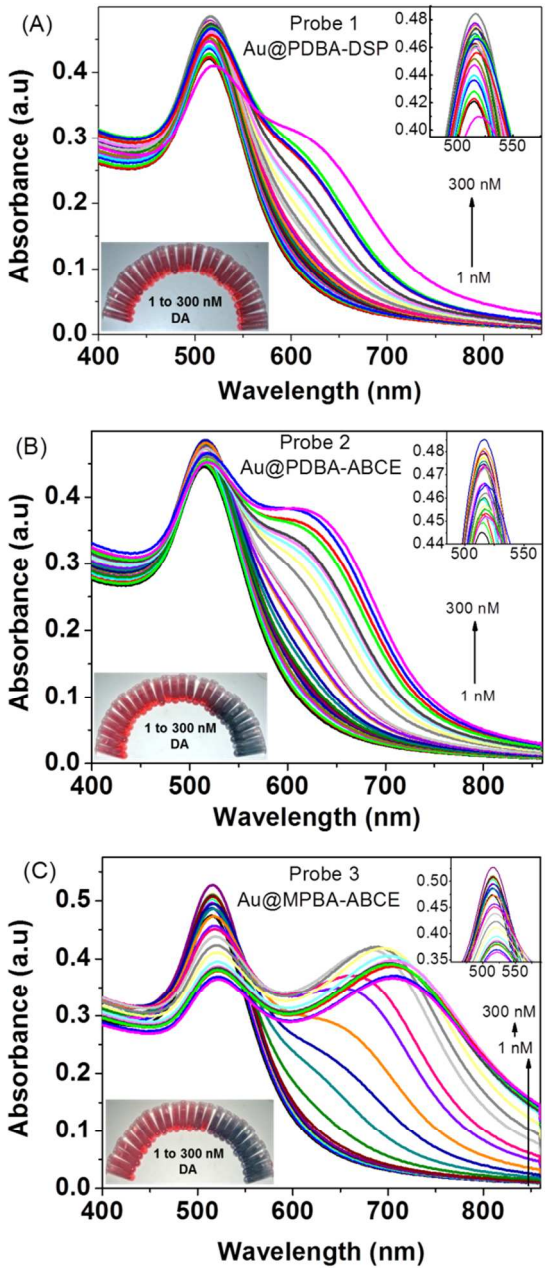

Fig. 2 UV-vis absorption spectra of different nanoprobes in the presence of 1 to 300 nM DA. (A) Probe 1, (B) Probe 2, and (C) Probe 3. Insets are the corresponding colorimetric visualization pictures and zoom-in plots at low DA concentrations.

When a very low concentration of DA was added into the aqueous suspension of the nanoprobes (< 40 nM), the characteristic SPR peak of Au NPs at 514 nm slightly increased in intensity and also broadened to some extent. Moreover, a slight red-shift occurred in the peak, and the suspension color changed from the wine red to orange red, and then purple red with the increase of DA concentration in the solution under test. These phenomena can be well explained by the slight increase in the

View Article Online
DOI: 10.1039/C5TB00495K

particle size upon the addition of DA (Figure 3), as indicated by the DLS measurements (Figures S1-S3), which was caused by the adsorption of DA molecules on Au NPs.[20] *It is noted that here the particles mean the Au NPs together with molecules (ligands) coated on them, not just Au NPs themselves.* Since the DA concentration is very low, such an increase in the particle size cannot lead to obvious aggregation of Au NPs. It is believed that charge transfer (CT) could take place from the Au NPs to the adsorbed DA molecules, leading to the tiny red-shift of the absorption peak at 514 nm since the N_e in Au NPs decreased.[23] As for the corresponding color change, it is mainly because of the quantum color effect due to the slight increase in the particle size.[24]

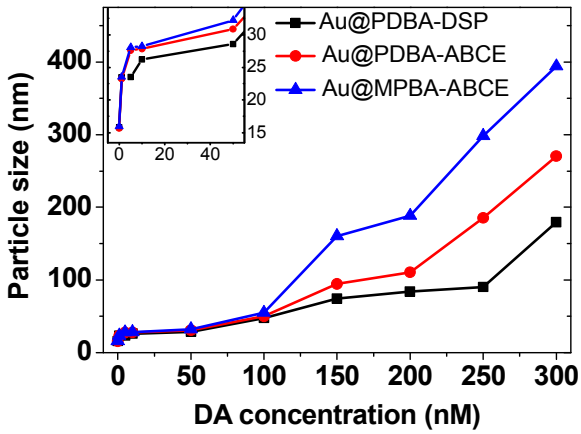

Fig. 3 Calibration plot between DA concentration and particle size for different nanoprobes. Inset is the zoom-in plot at low DA concentrations.

The particle size kept increasing (Figures 3 and S1-S3) upon further increase in the DA concentration (> 40 nM), gradually leading to the aggregation of Au NPs and, thus, a decrease in the concentration of Au NPs. As a result, the peak at 514 nm started to decrease in intensity as the SPR transverse peak is mainly dependent on Au concentration. Meanwhile, further obvious red-shift in the peak could be observed (Figure 2), which is mainly caused by the increase in the size of Au NPs core due to the aggregation, as well as the above CT process. Accordingly, the color turned to violet blue, blue, and finally to dark blue with the increase of DA concentration. In the meantime, an additional peak appeared at longer wavelength around 700 nm owing to the aggregation for Probe 3 and around 650 nm for Probe 1 and Probe 2, which is the SPR longitudinal mode and is weak in nature as compared with the transverse mode.[25] On the opposite to the amplitude change for the transverse peak, it increased with increasing DA concentration for the longitudinal peak, as it is sensitive solely to the particle size, not to the Au concentration. When the DA concentration was very high, however, the peak intensity for both the longitudinal and transverse modes decreased again, which was due to the precipitation of large sized aggregates.[26]

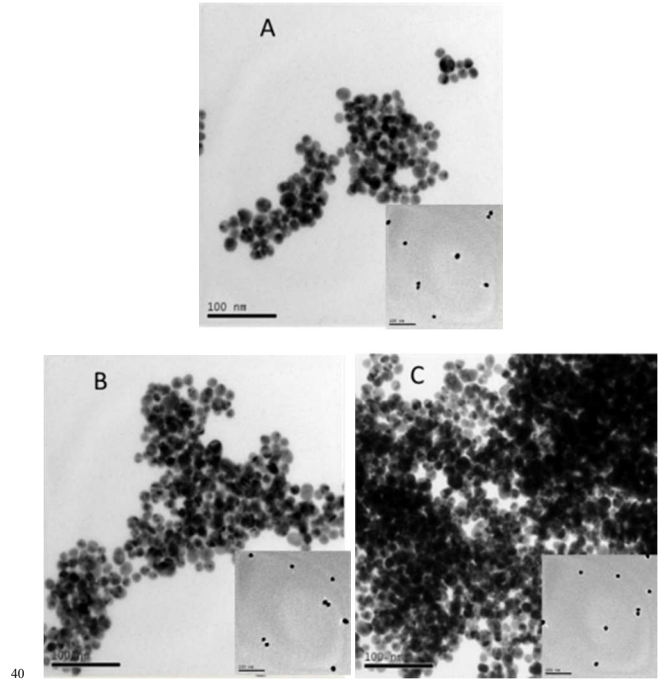

Fig. 4 TEM images of different nanoprobes with the presence of 150 nM DA: (A) Probe 1, (B) Probe 2 and (C) Probe 3. Insets show the corresponding images without the DA. Scale bar in all the images is 100 nm.

The observed aggregation of Au nanoprobes was confirmed by TEM images. Without the addition of DA molecules, only the isolated, monodispersed Au NPs could be observed for all the nanoprobes (insets of Figure 4). The aggregation occurred once the DA molecules were added into the aqueous suspension of nanoprobes (Figure 4). The higher the DA concentration, the more the aggregation took place. This agrees well with the change in particle size determined by DLS (Figures 3 and S1-S3).

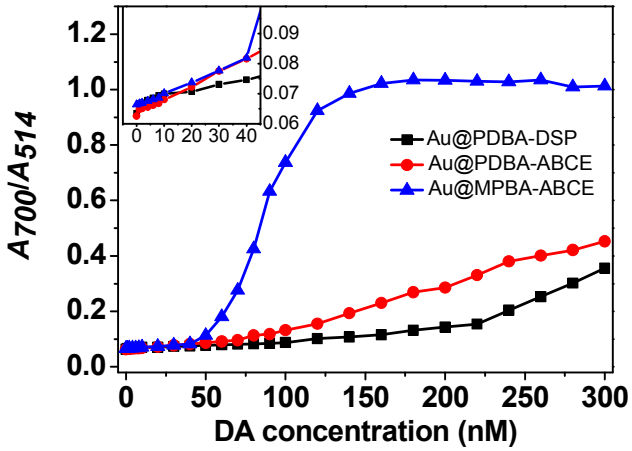

Fig. 5 Calibration plot between DA concentration and A_{700}/A_{514} peak ratio for the different nanoprobes. Inset is the zoom-in plot at low DA concentrations.

Since the colorimetric detection of DA is closely related to both the transverse and longitudinal peaks, ratio of the absorbance between them (A_{700}/A_{514}) was used to further evaluate the detection performance of the nanoprobes. Albeit the longitudinal peak for Probe 1 and Probe 2 is around 650 nm

View Article Online
DOI: 10.1039/C5TB00495K

instead of 700 nm, here the A_{700}/A_{514} ratio is used for all the three nanoprobes rather than A_{650}/A_{514} as they should have the same change trend. It is found that the A_{700}/A_{514} ratio increases with the increase of DA concentration in the suspension (Figure 5). When the DA concentration was comparatively low, the A_{700}/A_{514} ratio was proportional to the DA concentration, though the threshold value was different for different nanoprobes (about 100 nM for Probe 1, 70 nM for Probe 2, and 40 nM for Probe 3). Above this threshold value, the increase in the amplitude of A_{700}/A_{514} ratio became larger and larger. For Probe 3, it eventually tended to be constant, possibly due to the precipitation of large sized aggregates.

By using the values of A_{700}/A_{514} ratio for the control sample (without DA) and the one with noticeable change, the *LOD* for different Au nanoprobe was calculated to be 6.3 nM (S/N = 2.10, Probe 1), 6.2 nM (S/N = 2.07, Probe 2) and 6.0 nM (S/N = 2.01, Probe 3), respectively.[27] If it was determined with S/N ≈ 3, the *LOD* was about 117 nM for Probe 1, 66 nM for Probe 2, and 46 nM for Probe 3. It is noted that the *LOD* can be further improved greatly, even to be lower than 1 nM, by adding a certain amount of DA to the stock nanoprobe suspension in advance (for instance, about 240 nM for Probe 1, 100 nM for Probe 2, and 60 nM for Probe 3).[21] All these values were lower than or equivalent to the basal DA level of 0.01 to 1 μM,[2] indicating the obtained nanoprobes can be used for the *in-vivo* DA analysis.

3.2 Response time

The respective absorption amplitude at the wavelength of 514 nm and 700 nm with respect to the time was used to evaluate the response time for the three nanoprobes. For the control experiments (i.e., the probes with the presence of water, but without DA), no obvious change can be observed during the whole experiments. After adding 20 μL of 45 μM DA (300 nM of final concentration), as shown in Figure 6(a–b), the peak intensity at 514 nm slowly decreased for Probes 1 and 2, and the one at 700 nm slowly increased. As for Probe 3, it is noted that the peak intensity at 514 nm decreased sharply in the presence of DA for the first 10 s and then increased until the time reached 20 s, and eventually decreased thereafter; while the one at 700 nm increased in all cases although some fluctuation can be observed. The fluctuations in the absorbance peak intensity at 700 nm at around 100 s with respect to time might be due to the formation of inhomogeneous Au NPs after adding the DA molecules. Considering the changes in the peak intensity at both 514 nm and 700 nm, thus, the color change could be observed in about 40 s after adding DA for Probe 1 and about 2 s for Probe 2. Noticeably, the color changed from wine red to blue in about tens of ms for Probe 3. It is noted that the response time for all the three nanoprobes is much faster than the reported value of minutes.

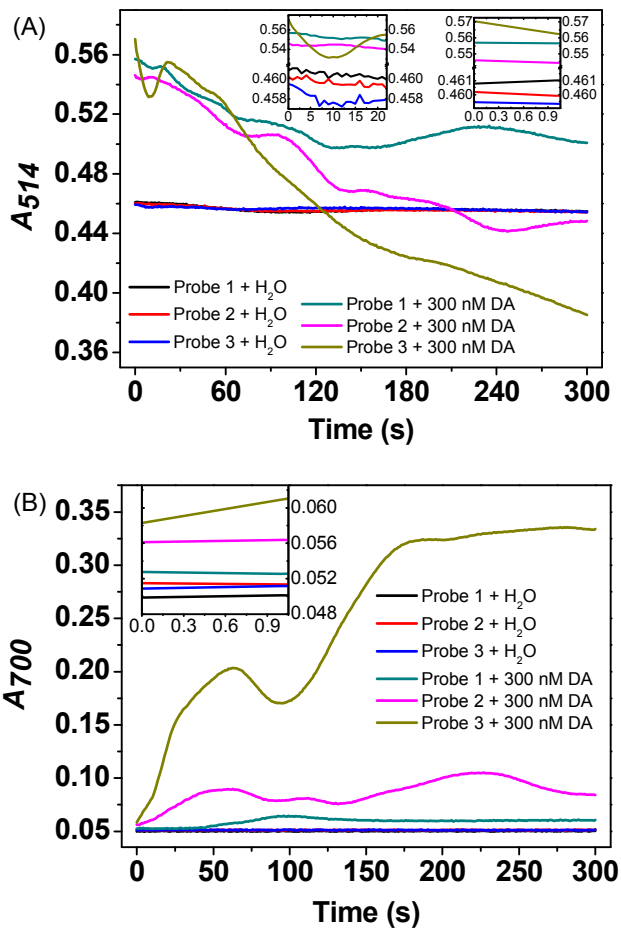

Fig. 6 Change of absorption intensity with time at the wavelength of (A) 514 nm and (B) 700 nm for different nanoprobes. Insets are those in intial stage.

3.3 Colorimetric detection mechanism

The phenomena discussed above can be elucidated in terms of the detection mechanism (Schemes 2 & S1). The DA molecules can be adsorbed onto the particle surface once they are added into the probe suspension, leading to the increase of particle diameter with the increasing DA concentration and, thereby, changes in other properties. The catechol group of DA interacts with the ligand bearing boronic group (PDBA or MPBA), and the amine group of DA interacts with the ligand of DSP or ABCE. Accordingly, the mechanism can be studied in detail by using the model of electric double layer (EDL).

View Article Online
DOI: 10.1039/C5TB00495K

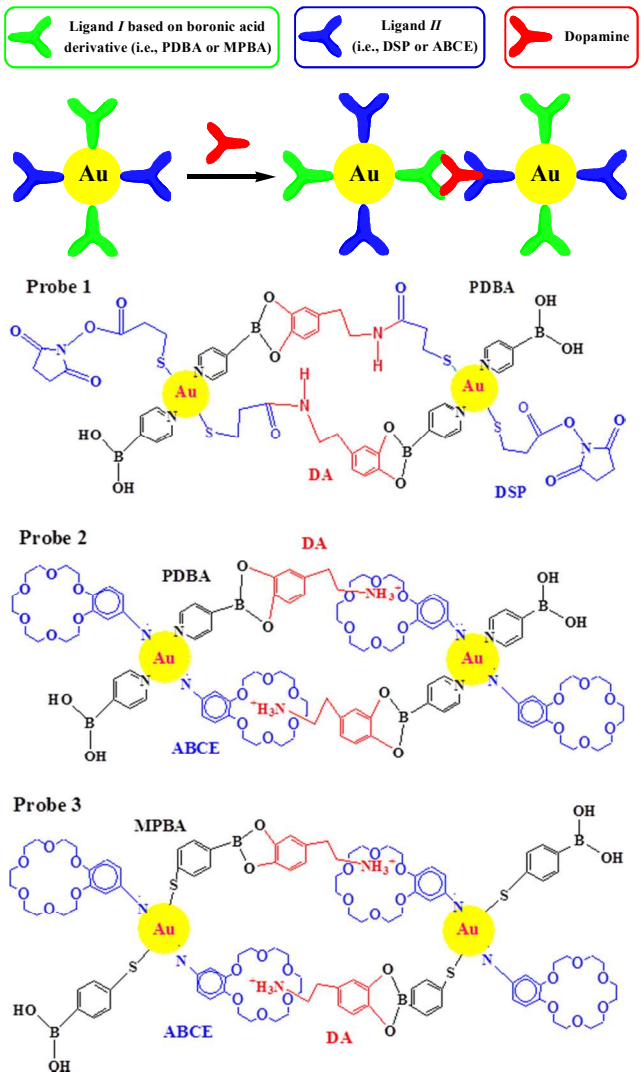

Scheme 2 Colorimetric detection of DA using different functionalized Au nanoprobes: Au@PDBA-DSP, Au@PDBA-ABCE and Au@MPBA-ABCE. Top schematic diagram shows the detection mechanism, and the bottom ones are those for the aggregates of three different nanoprobes with the presence of DA.

The colloidal Au NPs lose their stability upon the DA addition due to the EDL disturbance, and aggregation can thus occur,[23] which are closely related to the changes in pH and zeta potential. Without the presence of DA, these three nanoprobes have almost the same zeta potential and pH value (Figure 7 a & b). Once upon the addition of DA into the probe suspension, the zeta potential became more negatively and the pH value increased gradually. Since the DA molecule has both proton accepting amine group (pKa = 8.89) and proton donating dihydroxyl group (pKa = 10.5), the changes in the zeta potential and pH value are dependent on which functional group is involved in the interactions with Au NPs. The zeta potential would become more negatively and pH value would increase as well, if only the amine group is involved; while the zeta potential would become more positively and pH value would decrease, if only dihydroxyl group contributes to bonding.[28] In the proposed dual molecular recognition systems, it is suggested that both the amine and dihydroxy groups are involved. According to obtained results (Figure 7 a & b), thus, the contribution from the amine group is more than that from the dihydroxyl group. This is reasonable since the DA used here is hydrochloride, for which the amine group is positively charged. This may explain the above-discussed decrease in N_e caused by the charge transfer from Au NPs to DA. It can be further confirmed by the decrease in surface charge density (σ) for different nanoprobes upon the addition of DA (Figure 7c), calculated by using Gouy–Chapman model.[29]

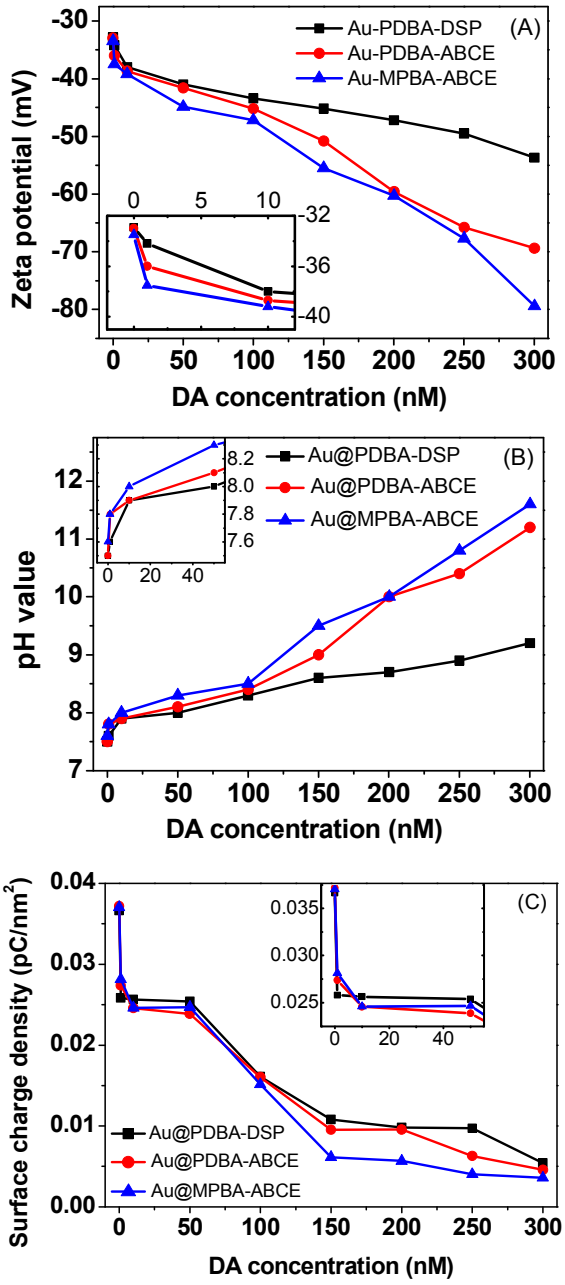

Fig. 7 Calibration plots between DA concentration and (A) zeta potential, (B) pH value, and (C) surface charge density for different nanoprobes with 1 to 300 nM DA. Insets are the zoom-in plots at low DA concentrations.

It is noted that Probe 3 exhibits the largest changes for all the aforementioned phenomena (color, absorption peak amplitude and shift, A_{700}/A_{514} ratio, particle size and aggregation, and response time), followed by Probe 2, and Probe 1 has the least changes, which can also be explained by the above mechanism.

View Article Online
DOI: 10.1039/C5TB00495K

All the nanoprobes have dual molecular recognition ligands, which make them exhibit high *LOD*, as discussed above. Both Probe 1 and Probe 2 have PDBA ligand molecule interacting with the catechol group of DA. It is the amine-reactive succinimidyl ester moiety in DSP ligand that reacts with the amine group of DA for Probe 1, and it is the crown moiety in ABCE ligand that interacts with the amine group of DA for Probe 2. In the former the chemical reaction occurs so as to form the peptide bond that links DA molecule with the nanoprobe; while in the latter the hydrogen atoms in the amine group of DA (actually protonated amine, i.e., totally three hydrogen atoms) are cross linked with the six oxygen atoms of crown ether moiety via hydrogen bonding.[30-32] Under mild conditions (like those used here), it is believed that the formation of hydrogen bonding can undertake more efficiently, faster and easier than a chemical reaction occurs. The difference between the interaction of grafting group and Au for DSP (thiol group) and ABCE (amino group) can be ignored in this case, albeit the former may be slightly stronger than the latter. Thus, Probe 2 exhibits better performance than Probe 1.

The reason that Probe 3 shows better performance than Probe 2 is that they have different ligand molecule that reacts with the catechol group of DA, although both of them have ABCE as the ligand interacting with the amine group of DA. The interaction between grafting group and Au for MPBA (thiol group) is much stronger than that for PDBA (nitrogen atom in pyridine moiety). In addition, the acidity of MPBA may be slightly stronger than that of PDBA since the former contains phenyl ring and the latter contains pyridine ring, which may also contribute to the improved performance of Probe 3.

3.4 Detection selectivity

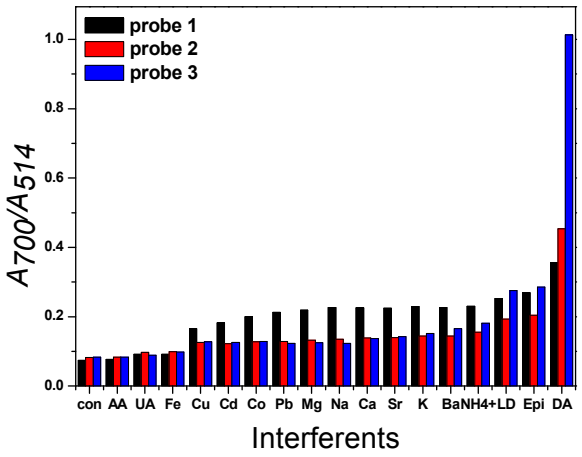

Fig. 8 The column graph for A_{700}/A_{514} ratio changes by adding DA and some other interferents into the three different nanoprobes.

To study the selectivity of DA detection for the obtained nanoprobes, excess amount of interferents (1000-fold) were added into the system, such as AA, UA, LD, epinephrine and some other metal ions. The visualization pictures for different nanoprobes are shown in Figures S4-S6. For all the three nanoprobes, the DA gives rise to much higher response (here the A_{700}/A_{514} ratio) than any of the interferents (Figure 8). A tiny change can also be observed for some interferents, either due to their weak interaction with crown ether (such as LD, NH_4^+ and the metal ions like Mg^{2+}, Na^+, Ca^{2+}, Sr^{2+}, K^+ and Ba^{2+}) as their atomic radius is almost the same as the size of crown cavity (260~320 pm),[32] or due to coordination bonding with boronic acid group (such as LD, epinephrine and the hexahydrates of transition metal ions like Fe^{2+}, Co^{2+} and Cu^{2+}).[33] Moreover, both AA and UA can cause very little change in the A_{700}/A_{514} ratio for all the three nanoprobes, which is due to the repulsion between negatively charged particle surface and anionic AA and UA (Figure 8).[34] Thus, all of the nanoprobes exhibit good detection selectivity. Based on the above discussion, again, Probe 3 is the highest, followed by Probe 2, and Probe 1 is the lowest.

4. Conclusions

In summary, we have successfully synthesized Au nanoprobes that can be used for highly sensitive and selective colorimetric detection of DA with fast response. The *LOD* of the Au nanoprobes can reach nanomolar levels, which is lower than or equivalent to the basal DA levels of 0.01 to 1 μM. Moreover, the response time can be about tens of ms for Probe 3, which is much faster than the reported values of the same type probes. Probe 3 exhibits very high detection selectivity even in the presence of 1000-fold excess of many different interferents like metal ions, UA and AA. Thus, the obtained Au nanoprobes can merit the *in–vivo* DA analysis, as such method has already been applied for the DA detection in the rat brain, although it cannot detect multiple analytes simultaneously since there is no any peak separation in the spectra. Because of the simplicity in operation and instrumentation of the colorimetric method, this work may afford a feasible, fast approach for detecting and monitoring the DA levels in physiological and pathological systems.

Acknowledgements

This work was supported by National Research Fund for Fundamental Key Projects No. 973 (2011CB933200).

Notes and references

[a] *Key Laboratory of Nanosystem and Hierarchical Fabrication, National Center for Nanoscience and Technology, Beijing 100190, China. Fax: 86 10 6265 6765; Tel: 86 10 8254 5655; E-mail: het@nanoctr.cn and zhangxh@nanoctr.cn*

[b] *University of Chinese Academy of Sciences, Beijing 100049, China*

† Electronic Supplementary Information (ESI) available: Schematic diagrams for the colorimetric detection of DA using functionalized Au probes, the interaction between DA and the respective Au NPs modified with different ligand molecules as well as together on citrate capped Au NPs, table for the FT-IR results, DLS data for different probes with different amount of DA, colorimetric visualization of different probes with the presence of DA and interferent foreign molecules, and a list for the concentrations of DA used in the system under test. See DOI: 10.1039/b000000x/

1 A. M. Krstulovic, Quantitative analysis of catecholamines and related compounds, Ellis Horwood, Chichester, 1986.
2 G. Dernick, G. Alvarez de Toledo and M. Lindau, Electrochemical methods in neuroscience, Chapter 15, CRC Press, Boca Raton (FL), 2007.
3 C. Wang, R. Yuan, Y. Chai, S. Chen, F. Hu and M. Zhang, *Anal. Chim. Acta*, 2012, **741**, 15.
4 K. Kwak, S. Senthil Kumar and D. Lee, Nanoscale, 2012, **4**, 4240.
5 M. R. H. Nezhad, J. Tashkhourian and J. Khodaveisi, Anal. Methods, 2010, **2**, 1263.

View Article Online
DOI: 10.1039/C5TB00495K

6 X. L. Zhu, P. N. Shaw and D. A. Barrett, Anal. Chim. Acta, 2003, **478**, 259.
7 N. Li, J. Z. Guo, B. Liu, H. Cui, L. Q. Mao and Y. Q. Lin, Anal. Chim. Acta, 2009, **645**, 48.
8 M. A. El-Sayed, Acc. Chem. Res., 2001, **34**, 257.
9 A. C. Templeton, W. P. Wuelfing and R. W. Murray, *Acc. Chem. Res.*, 2000, **33**, 27.
10 Y. G. Sun and Y. N. Xia, *Analyst*, 2003, **128**, 686.
11 H. Ditlbacher, J. R. Krenn, N. Felidj, B. Lamprecht, G. Schider, M. Salerno, A. Leitner and F. R. Aussenegg, *Appl. Phys. Lett.*, 2002, **80**, 404.
12 J. J. Feng, H. Guo, Y. F. Li, Y. H. Wang, W. Y. Chen and A. J. Wang, *ACS Appl. Mater. Interfaces*, 2013, **5**, 1226.
13 J. D. Larkin, K. A. Frimat, T. M. Fyles, S. E. Flower and T. D. James, *New J. Chem.*, 2010, **34**, 2922.
14 Y. J. Jang, J. H. Jun, K. M. K. Swamy, K. Nakamura, H. S. Koh, Y. J. Yoon and J. Yoon, *Bull. Korean Chem. Soc.*, 2005, **26**, 2041.
15 J. K. W. Chui and T. M. Fyles, *Supramol. Chem.*, 2008, **20**, 397.
16 H. Cao and M. D. Heagy, *J. Fluoresc.*, 2005, **14**, 569.
17 Z. Guo, I. Shin and J. Yoon, *Chem. Commun.*, 2012, **48**, 5956.
18 J. Yoon and A. W. Czarnik, *Bioorgan. Med. Chem.*, 1993, **1**, 267.
19 H. C. Lee, T. H. Chen, W. L. Tseng and C. H. Lin, *Analyst*, 2012, **137**, 5352.
20 L. Liu, S. J. Li, L. L. Liu, D. H. Deng amd N. Xia, *Analyst*, 2012, **137**, 3794.
21 B. Kong, A. W. Zhu, Y. P. Luo, Y. Tian, Y. Y. Yu and G. Y. Shi, *Angew. Chem. Int. Ed.*, 2011, **50**, 1837.
22 K. C. Grabar, R. G. Freeman, M. B. Hommer and M. J. Natan, *Anal. Chem.*, 1995, **67**, 735.
23 S. K. Ghosh and T. Pal, *Chem. Rev.*, 2007, **107**, 4797.
24 Y. Q. He, S. P. Liu, L. Kong and Z. F. Liu, *Spectrochim. Acta A*, 2005, **61**, 2861.
25 G. Leveque and R. Quidant, *Opt. Express*, 2008, **16**, 22029.
26 R. A. Puebla, E. Arceo, P. G. Goulet, J. Garrido and R. F. Aroca, *J. Phys. Chem. B*, 2005, **109**, 3787.
27 A. Shrivastava and V. B. Gupta, *Chron. Young Sci.*, 2011, **2**, 21.
28 J. L. Berfield, L. C. Wang and M. E. A. Reith, *J. Biol. Chem.*, 1999, **274**, 4876.
29 T. I. Zohdi, Electromagnetic Properties of Multiphase Dielectrics, Springer Verlag Berlin: Heidelberg, 2012.
30 A. Robertson and S. Shinkai, *Coord. Chem. Rev.*, 2000, **205**, 157.
31 M. F. Paugam, L. S. Valencia, B. Boggess and B. D. Smith, *J. Am. Chem. Soc.*, 1994, **116**, 11203.
32 A. Spaeth and B. Koenig, *Beilstein J. Org. Chem.*, 2010, **6**, 32.
33 N. SeethaLekshmi and V. R. Pedireddi, *Inorg. Chem.*, 2006, **45**, 2400.
34 M. M. Zaresh, *J. Appl. Sci.*, 2008, **8**, 3654.

View Article Online
DOI: 10.1039/C5TB00495K

Fast, sensitive and selective colorimetric gold bioassay for dopamine detection

Sivakumar Palanisamy, [a,b] Xuehua Zhang, *[a] and Tao He *[a]

[a] Key Laboratory of Nanosystem and Hierarchical Fabrication, National Center for Nanoscience and Technology, Beijing 100190, China

[b] University of Chinese Academy of Sciences, Beijing 100049, China

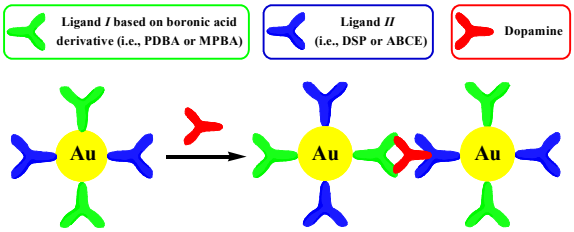

A highly sensitive and selective colorimetric biosensor for dopamine has been developed by using double molecular recognition modified Au nanoparticles.